SEVENTH FRAMEWORK PROGRAMME
THEME FP7-ICT-2007-2
Information and Communication Technologies

Project # 224197 – TUMESA

MEMS Tuneable Metamaterials for Smart Wireless Applications

Deliverable 3.6

"Test and evaluation of the novel steering leaky-wave antenna at a radar front end level"

Contractual Date of Delivery to the CEC: September 30th, 2011

Actual Date of Delivery to the CEC: September 30th, 2011

Author(s): Ghayath EL HAJ SHHADE, Frantz BODEREAU

Participant(s): AUTOCRUISE

Workpackage: WP3, System Implementation to Wireless Applications

Est. person months: 10

Security: PU

Nature: R/P

Version: 1.0

Total number of pages: 14

Abstract:

Following the design, simulation and optimization of the coupling leaky-wave antenna (CLWA) at Autocruise in the frame of TUMESA, an antenna prototype has been fabricated and measured. The antenna demonstrated the capability of fixed frequency beam steering by testing different periodic perturbations implemented on separate silicon chips. Overall, the antenna demonstrated good performances and hence can be mounted on a 77-GHz automotive radar front-end. However, to realize this, several issues in terms of packaging and integration capability of the antenna must be taken into account.

Keyword list: LWA, fixed-frequency beam steering, MEMS, integration capability, 77-GHz automotive radar front-end.

Executive Summary

In this deliverable, the measurement results of the coupling leaky-wave antenna in anechoic chamber are presented. Then, the capability of fixed-frequency electronic beam steering is tested and evaluated. Finally, we present the requirements to be taken into account while implementing the antenna within a 77-GHz radar front-end.

Full description of deliverable content

1 Test and evaluation of the coupling leaky-wave antenna in anechoic chamber

1.1 Introduction

In this section, the measurement results of the CLWA in anechoic chamber are presented. The measurements took place at IETR in June 2011. For a detailed description of the test procedure, along with the measurement results of the tested configurations, please refer to Deliverable D2.4.

1.2 Measurement setup

The CLWA prototype mounted in the measurement chamber is shown is Figure 1.

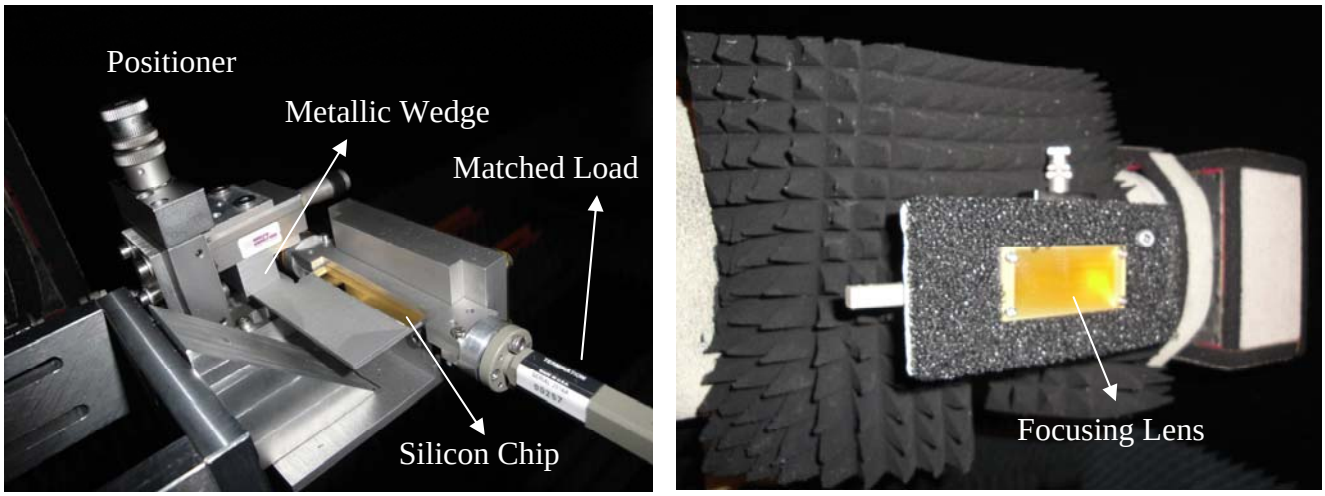

Figure 1 – CLWA prototype in the measurement chamber (UR1)

The perturbations etched on the metal layer on top of the silicon substrate (Figure 2) are coupled to the dielectric rod inside the metallic waveguide via a 300µm-width slot (Figure 3). The chip is glued on a metallic plate and fixed with screws into the positioner via a metallic wedge. The antenna is excited at one end with a WR10 waveguide, and connected to a matched load on the other end. This is realized using a WR10-to-microstrip-to-waveguide transition at both sides of the packaging waveguide (cf. D3.4).

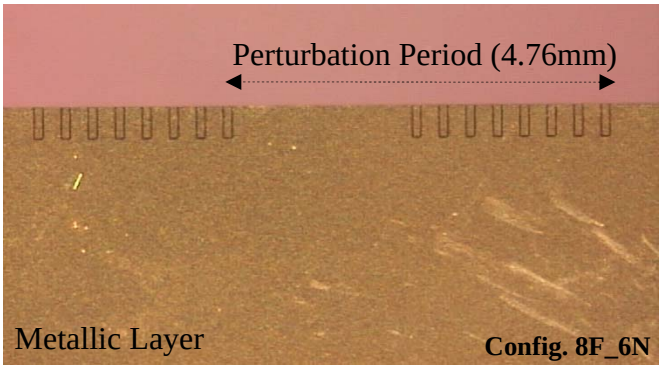

Figure 2 – A fabricated silicon chip with etched perturbations (Top View)

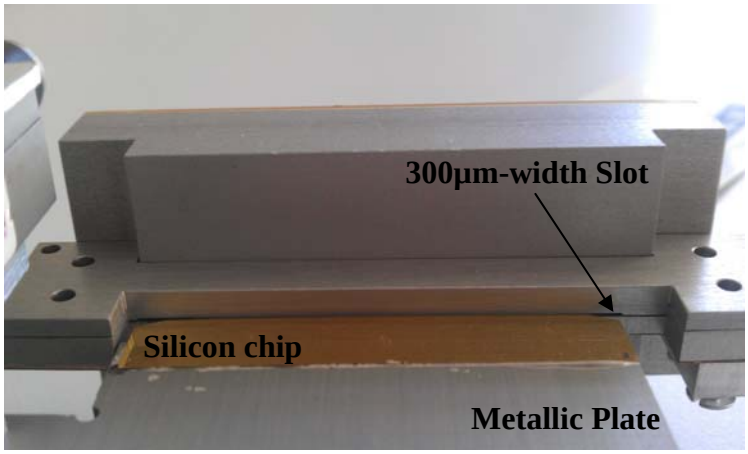

Figure 3 – The 300µm-width slot

1.3 Tested configurations

The CLWA prototype was measured in the anechoic chamber at UR1 in the [72 GHz -80 GHz] frequency band. The measurements focused on four main configurations as summarized in Table 1.

Configuration	Code	Period length [mm]	Azimuth beam angle [°] @ 76.5 GHz / broadside
1	5F_6N	3.74	-12°
2	7F_5N	4.08	-5°
3	8F_6N	4.76	2°
4	8F_7N	5.1	5°

Table 1 – Measured configurations

1.3.1 Azimuth radiation patterns (5F_6N)

In this section, only the measurements of the 5F_6N configuration are presented.
The measured azimuth radiation patterns are shown in Figures 4.a & 4.b in the 72 - 80 GHz frequency band. We observe a good agreement with HFSS simulations at all frequencies notably when it comes to the angular position of the main beam. As expected, the measured beam angle at 76.5 GHz is 12° and the -3dB beamwidth is 7.5°. As for the sidelobe level, the latter increases at higher frequencies and the beam shape degrades as well.

Finally, we notice that the frequency scanning is relatively low, as the beam angle moves around 1° per GHz. This low value for frequency scanning illustrates one of the advantages of the CLWA in comparison with the silicon rod LWA structure which was investigated at the beginning of TUMESA project.

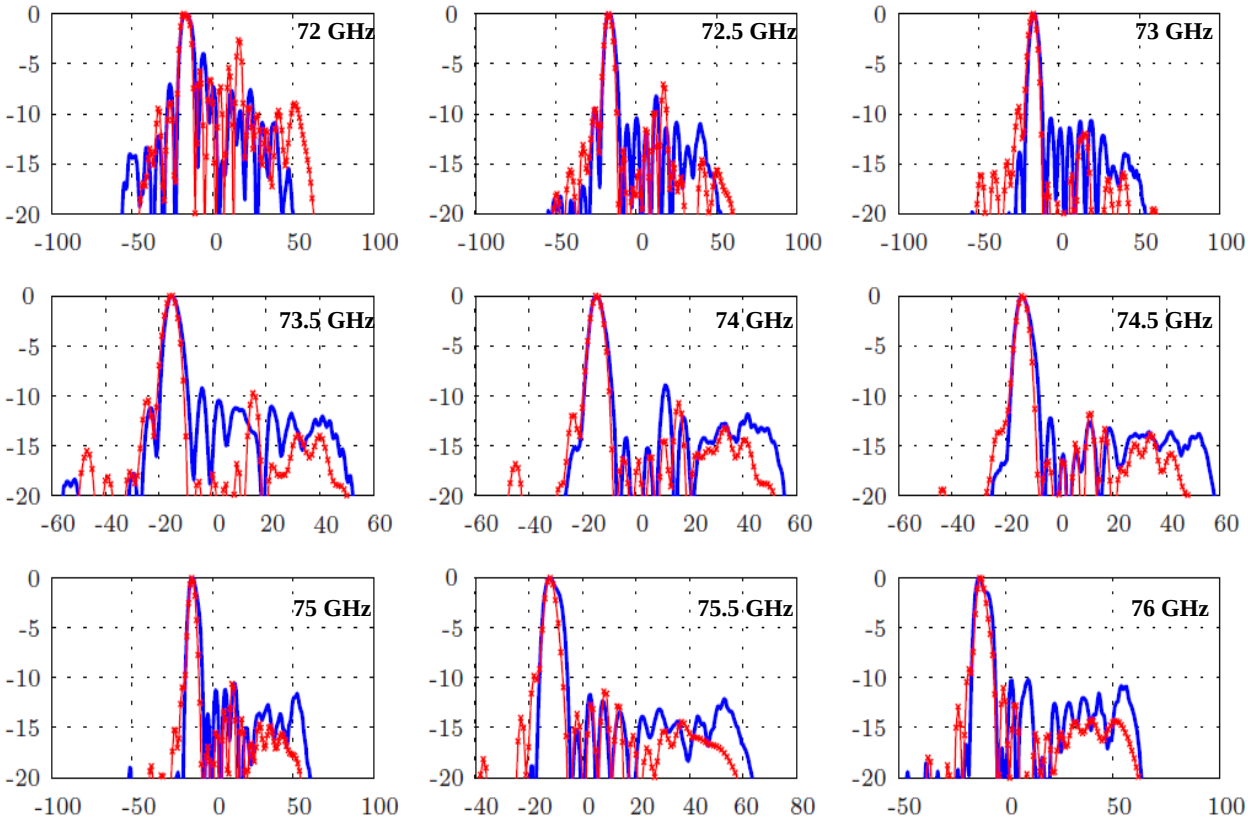

Figure 4.a. – Measured (Blue) and Simulated (Red) azimuth radiation patterns [dB] Vs azimuth angle [°] in the [72 GHz – 76 GHz] frequency band

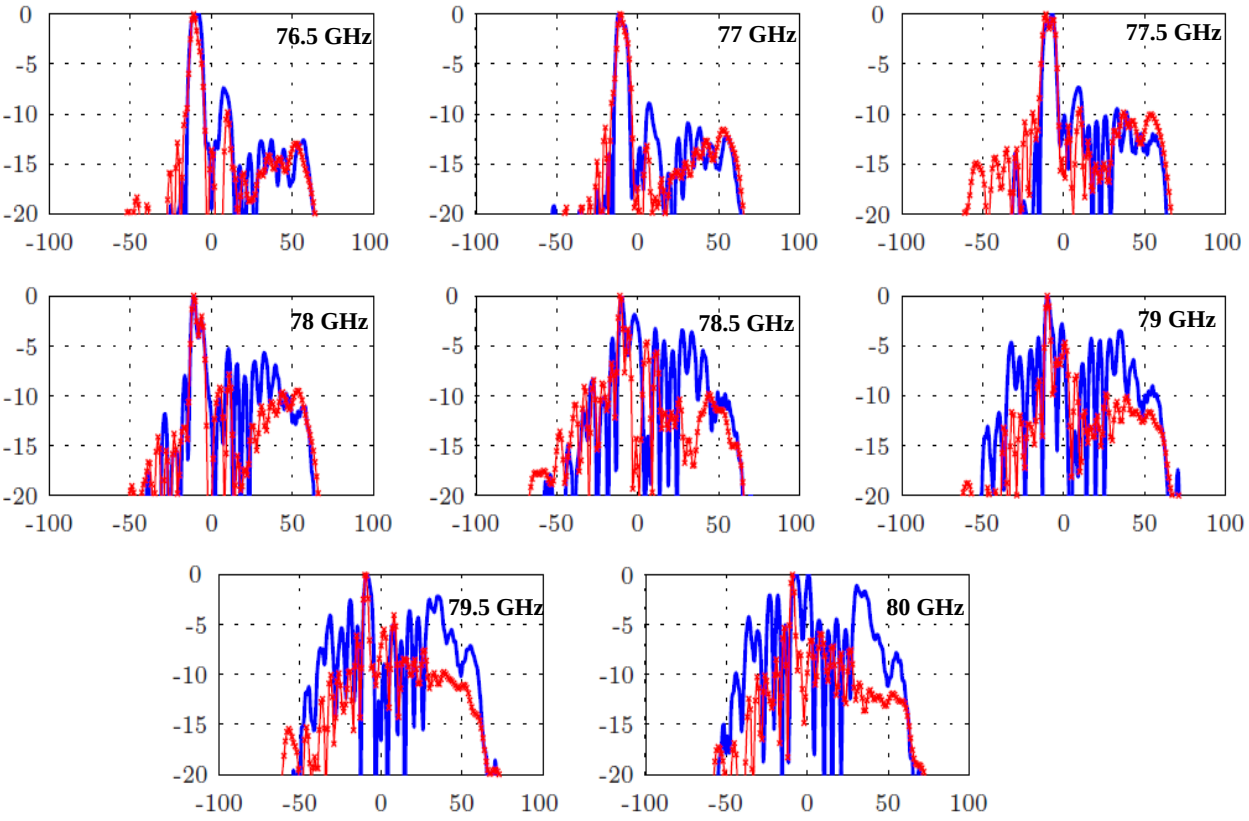

Figure 4.b. – Measured (Blue) and Simulated (Red) azimuth radiation patterns [dB] Vs azimuth angle [°] in the 76.5 GHz – 80 GHz frequency band

1.3.2 Scattering Parameters (5F_6N)

Both measured and simulated results are illustrated in Figures 5.a & 5.b in the 72 GHz – 80 GHz frequency band.

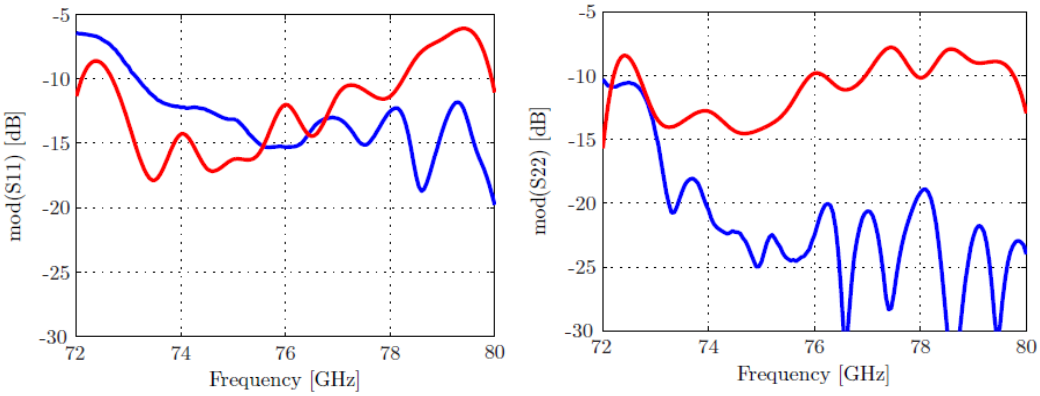

Figure 5.a – Measured (Blue) and Simulated (Red) $|S_{11}|$ [dB] (left) & $|S_{22}|$ [dB] (right) Vs Frequency [GHz]

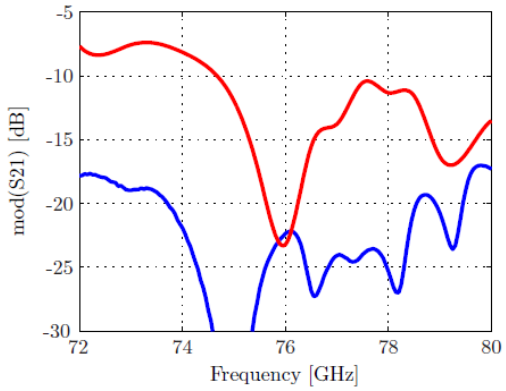

Figure 5.b – Measured (Blue) and Simulated (Red) $|S_{21}|$ [dB] Vs Frequency [GHz]

The measurements show that the $|S_{11}|$ is kept below -12 dB in the band of interest. The measurements results are even better than the simulations for the $|S_{22}|$, kept below -20 dB.
As for the transmission, the results are lower than the simulations in the frequency band. This can be explained by the losses in the WR10-to-microstrip-to-waveguide transitions on both ends of the antenna, the air gaps at both sides of the metallic support holding the dielectric rod, and the radiation influenced by the fabrication constraints.
Overall, from the matching/transmission points of view, the antenna operates well in the frequency band of interest.

1.3.3 Antenna gain (5F_6N)

Measured and simulated antenna gains are plotted in Figure 6 in the 75 GHz – 80 GHz frequency band. The gain is determined via the comparison method. As a reference, a standard gain horn (SGH) antenna is used. The gain for the antenna under test (AUT) is deduced from the comparison of the measured power levels.
The antenna gain is near 22 dBi in the 76.5 – 77 GHz region, as expected for a lens + source system.

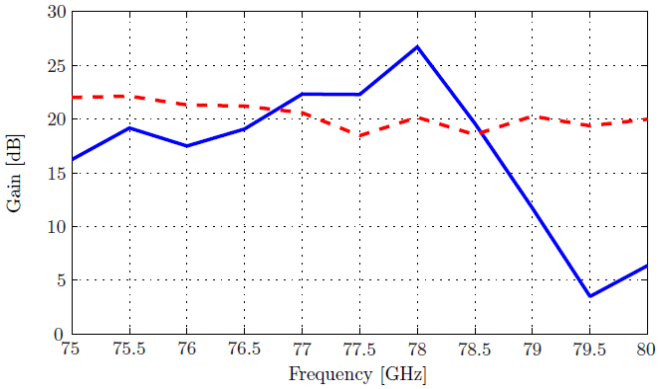

Figure 6– Measured (Blue) and HFSS Simulated (Red) antenna gain [dBi] Vs Frequency [GHz]

1.3.4 Effect of the coupling distance on the antenna performance (5F_6N)

The effect of the coupling distance on the antenna performance has been observed on both azimuth radiation patterns and S-parameters. In the first case, we tested three coupling distances with a step increment of 100µm in the 5F_6N configuration. According to measurements, this variation affects the sidelobe level: for frequencies below 76GHz, a better sidelobe level has been achieved with greater coupling distances whereas closer coupling distances provide better sidelobe performance for frequencies above 76 GHz.

As for the antenna performance in terms of S-parameters, it has been shown that the matching is kept below -10 dB for the $|S_{11}|$ and -15 dB for the $|S_{22}|$, even with great variations of the coupling distance e.g. from negligible to high coupling values. Thus, we can fairly say that the effect of the coupling distance on the matching is negligible. On the other hand, the transmission decreases when the coupling is increased. This can be explained by the leaky-wave radiation when the periodic perturbations etched on top of the silicon substrate are sufficiently coupled to the dielectric rod. All these measurement results are already reported in D2.4.

1.3.5 Effect of the position of the first strips (7F_5N)

We discussed in the previous deliverables the effect of the position of the first strips on the radiation pattern of the antenna and illustrated it with HFSS simulations. Hence, to validate it via measurements, we tested the antenna prototype with two perturbating chips, both in the 7F_5N configurations (same perturbation period c.f. Table 1) but with different positions for the first strips. Obviously, the same beam angle was obtained for both configuration (the perturbation period is kept unchanged) but with different sidelobe level performance. Consequently, it is possible to reduce the side lobe levels for each configuration within the design, i.e. by suitably choosing the position of the first strips. This point was studied in previous simulations, and now validated by measurements. Theses results have already been reported in D2.4.

1.3.6 Elevation Radiation Pattern (7F_5N)

The antenna was measured in the elevation plane in the 7F_5N configuration. The results are shown in Figure 7 at 76GHz for the correspondent azimuth beam angle.

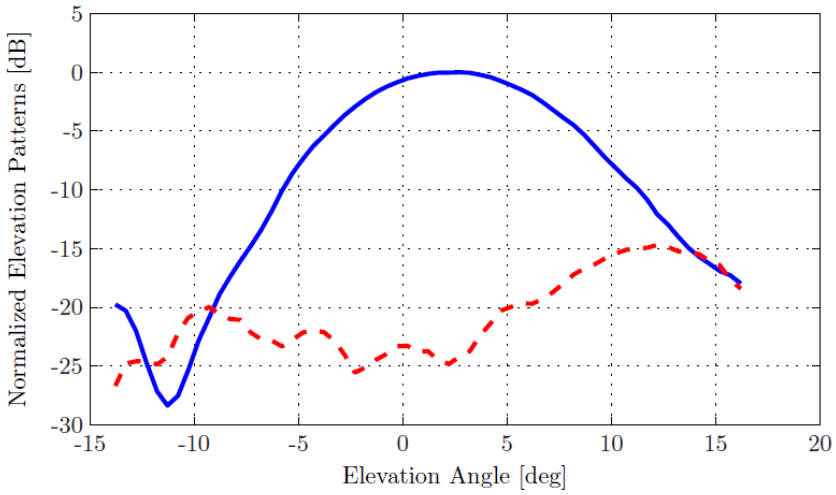

Figure 7 – Measured elevation radiation patterns [dB] Vs Elevation angle [°] @ 76 GHz.
Blue (Co-polarization), Red (Cross-polarization)

The main lobe is observed at 2.2°. This is due to a slight displacement of the radiating source with respect to the focal length of the lens.

1.3.7 Capability of fixed frequency beam steering

The same test procedures were applied to the four configurations in Table 1. Due to the limitation of space, we do not show them in this deliverable.
To validate the concept of fixed frequency beam steering, the measured radiation patterns of the four tested configurations are compared at 77GHz. The results are shown in Figure 8.

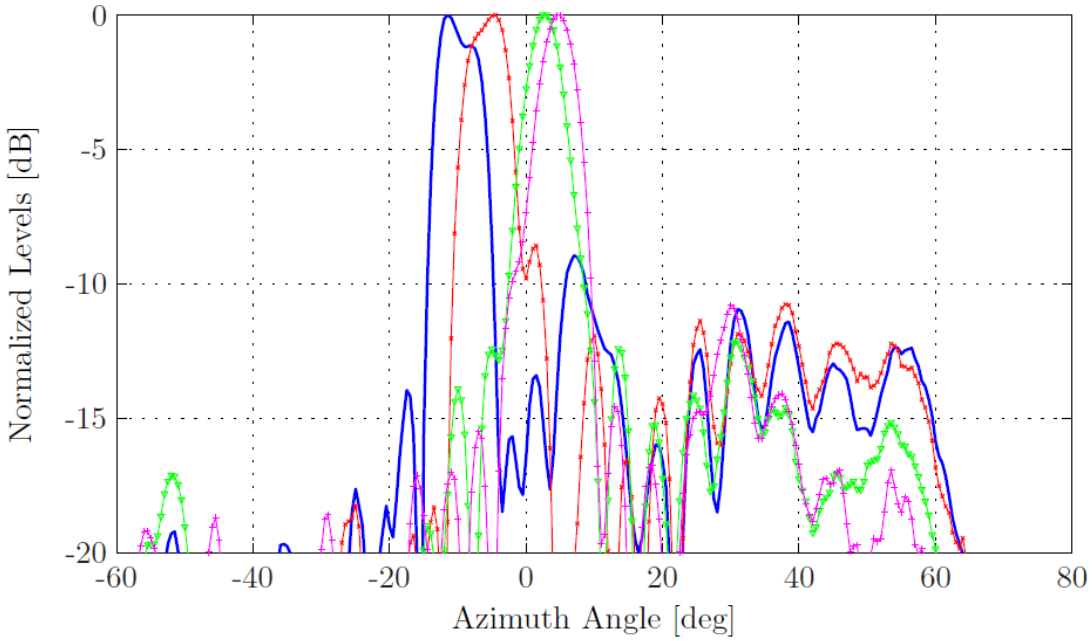

Figure 8 – Measured azimuth radiation patterns [dB] at 77GHz Vs azimuth angle [°] for each tested configuration

Referring to Table 1, we notice that the beam angle varies accordingly with the length of the perturbation period. This is true for all frequencies. In addition, the side lobe levels can be improved by optimizing the position of the first strips for each configuration.

1.4 Evaluation of the CLWA

We designed, simulated, optimized, fabricated and measured the coupling leaky-wave antenna. The prototype has been characterized and validated; the measurement results agree with the HFSS simulations, notably for the estimation of the azimuth angular position of the main beam.

The prototype capability of fixed-frequency electronic beam steering has been validated: for a periodic leaky-wave antenna, the beam angle varies accordingly with the length of the perturbation period (at a fixed frequency). In addition, the effect of the coupling distance and the lens on the antenna performances has been observed.

The side lobe levels can be improved with further optimization of the coupling distance, the position of the first strips for each chip configuration and finally by using non-uniform periodic configurations the modulate the antenna effective aperture.

Finally, the overall good performances achieved with this “passive” CLWA prototype (different chip configurations) open the door to the implementation of an “active” CLWA prototype where the perturbation period can be varied electronically via integration of MEMS switches on the silicon substrate to realize electronic beam steering.

2 Antenna implementation in 77-GHz automotive radar front-end

2.1 Introduction

In this section, we will show how the implementation of the antenna prototype will look like in 77-GHz automotive radar front-end. A synoptic presentation of the radar system with the scanning antenna is shown in Figure 9.

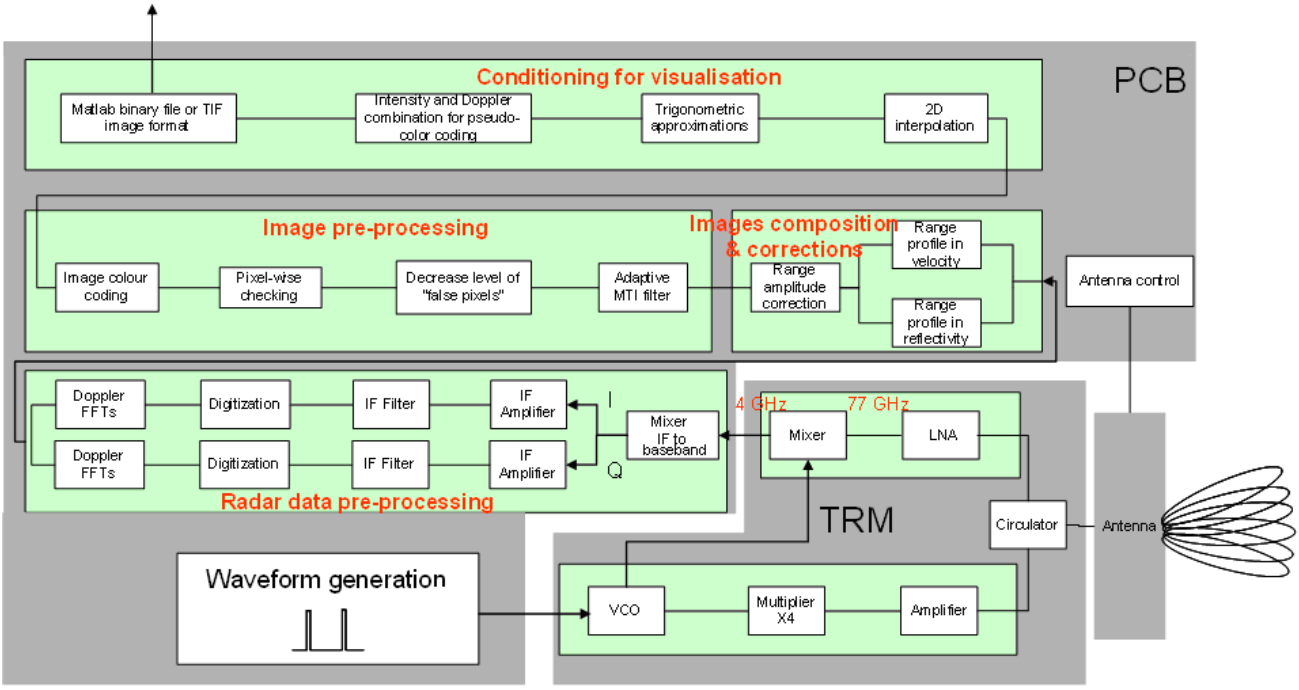

Figure 9 - Synoptic presentation of the radar system

2.2 Architecture of the RF transceiver

The architecture of the RF transceiver is directly related with the antenna concept. For example, the configuration shown in Figure 10 uses a bistatic architecture associated to an array of antenna elements to realize the beamforming in RX.

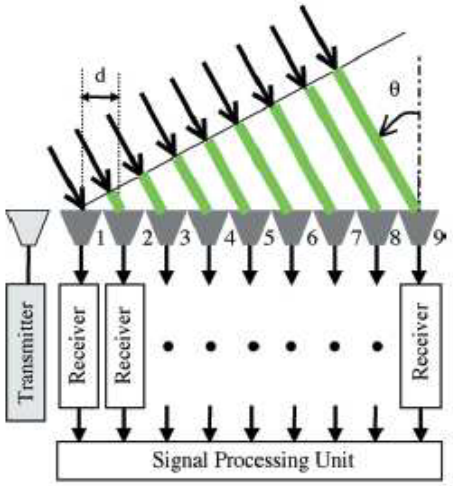

Figure 10 - multi-channel architecture [1]

Since a separate RX-channel is required for each antenna element, this approach exhibits high cost and is difficult to integrate using GaAs technology. This problem can be solved with the emergence of the new SiGe / CMOS technologies which offer the capability of higher integration and lower cost.

In our case, one of the advantages of the developed CLWA is that the beam scanning can be realized using a single antenna element. Therefore, only one RF-channel is required in RX and the RF transceiver can be realized in a simple monostatic architecture using GaAs technology (Figure 11).

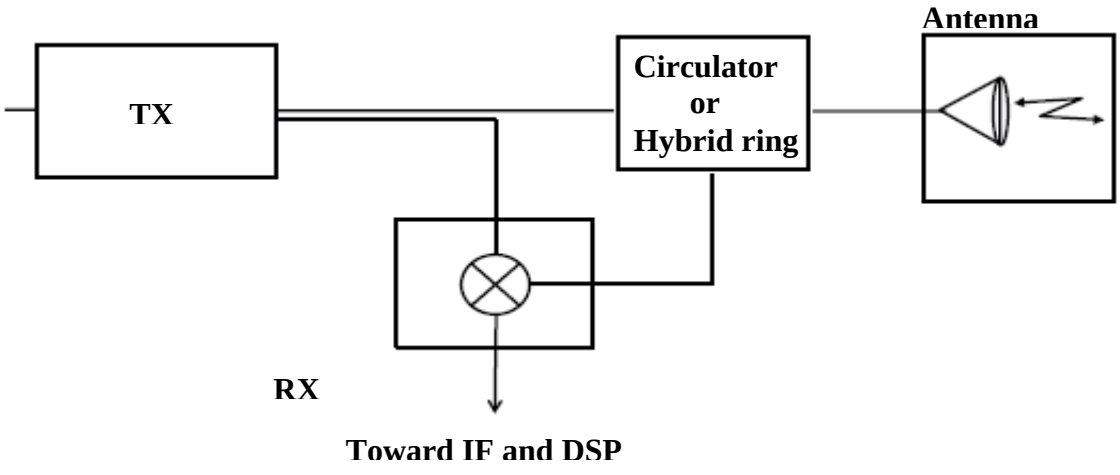

Figure 11 - Proposed transceiver architecture for the CLWA

The core of the RF transceiver is composed of MMICs operating at 77 GHz. The connection between the MMICs and the antenna is realized via RF substrate. As the antenna operates in monostatic mode, the transition between the transceiver and the antenna mainly affects the following performances:

- TX power,
- Noise factor in RX,
- Isolation between TX & RX,

Consequently, the transition losses and the matching have to be optimized with a low cost and compliant technology. For this reason, a waveguide (antenna side) / planar (transceiver side) transition has been developed in order to ensure the best interface with the transceiver (cf. D3.4).

2.3 Interconnection and packaging issues

The selection of the most suitable assembling and packaging technique for the antenna depends on the antenna & transceiver architectures and technologies. The main criteria are:

- Cost
- Integration capability
- Thermal dissipation
- RF performances in the temperature range
- Mechanical compliance between material versus temperature
- Maturity and reliability of the technologies
- Sensitivity versus process dispersion, assembling, …
- Leading time for the assembling
- Life time
- Protection versus external environment

Best compromises have to be found between these criteria. Some criteria are mandatory and no compromise can be accepted

2.3.1 Cost

The cost is a main criterion in the automotive industry. It is set to <200€ per unit and the antenna part has to be <20€. The RF part is a big contributor the radar cost. The latter depends on:

- Basic material: substrates
- Processes to realize the “component”
- Steps for the component assembling in the global structure
- Accuracy requirement of the assembling
- Lead time for all the processes and final integration
- Packaging if needed for environment protection

The priority must be given to simplicity which is not often easy. At the moment, the CLWA isn't suitable for commercialization as the cost needs to be improved to comply with the automotive mass production constraints.

2.3.2 Integration capability

The radar integration is mainly driven by the antenna dimensions. The latter must be kept below 100m x 60mm x 40mm. This requires a high integration level the following components:

- Integration of MMICs
- RF substrate to connect MMICs with antenna
- 3D transition between antenna and RF substrate
- DC components and lines for MMICs biasing
- antenna control

– antenna device
– global packaging

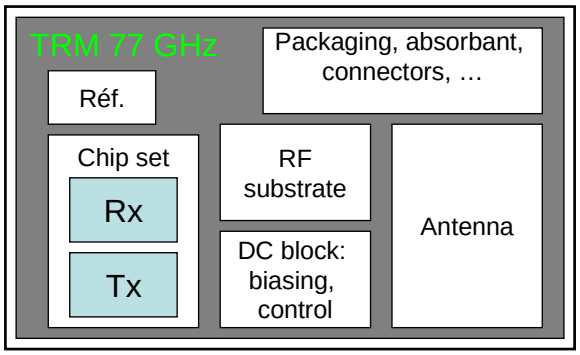

Figure 12- Integration of the RF components

Without taking into account the mechanical parts, the dimensions of the passive CLWA prototype (waveguide packaging + lens) are 84.4mm x 28mm x 33mm. If we take into account the WR-10 to microstrip transitions on both ends, the antenna size becomes 96.4mm x 29mm x 33mm. As for the active CLWA, extra size in the y-direction has to be considered for the biasing circuit of the MEMS switches.

2.3.3 Thermal dissipation

Thermal dissipation is a critical factor for high level integration issues: SiP, wafer level integration etc. The operating temperature range of the radar sensor is set according to standards from -40°C to 125°C and the storage temperature (no power) from -40°C to 130°C. MMICs are main contributors to power consumption (around 250 to 500 mA).
Consequently, the employed technology and the packaging technique must provide a good thermal dissipation coefficient.

2.3.4 Effect of the packaging on the antenna performance

The antenna integration in the radar system must be considered at the beginning of the development. Indeed, an antenna can have very good intrinsic performance however the latter can degrade significantly if the integration requires transitions with high losses and/or very narrow band of operation. Moreover, the addition of packaging for environmental protection could also affect the antenna efficiency (e.g. protection of the MEMS components in the "active" CLWA).
The antenna specification are deduced from the radar link budget: transition losses must be kept less than 1dB and matching below -15 dB in the frequency band of operation. This criterion has been taken into account during the development of the CLWA and validated by measurements.

2.3.5 Mechanical properties Vs temperature

The stacking of the different components (antenna, RF substrate, plate etc.) has to ensure good mechanical thermal expansion coefficient in the 3 axes. For example, a bad mechanical thermal expansion of the substrate in the z direction might create non flat and non regular ground continuity if the substrate is glued on a metallic plate. This effect is more problematic with large substrate dimensions, which is often the case with the antenna. Autocruise has the experience of reducing this effect while integrating the different components within the radar system.

2.3.6 Maturity and reliability of the technology

The technological choices must be coherent with the antenna concept (i.e. CLWA) and its integration and packaging process. In our case, GaAs technology seems to be a good choice due to its maturity, high performance and the simplicity of the transceiver architecture (1 RF-channel in RX).
Due to the enormous progress in chipset technology, future automotive radars will tend to use silicon-based technologies due to its high integration capabilities (especially with array antennas) and its low cost.

2.3.7 Sensitivity versus process dispersion, assembling, …

The antenna integration has to be robust versus technology, processes and assembling spread. Hence, worst cases have to be considered to analyze the antenna performance in its real environment and Monte Carlo simulations can be realized to see if the performance remains in the specified envelope. Several sensitivity issues regarding the CLWA have already been studied and reported in previous deliverables.

2.3.8 Leading time for the assembling

The leading time depends on the assembling and the steps required for the antenna integration within the radar system. This criterion impacts the cost of production. Thus, the priority is to reduce the assembling steps as much as possible in order to reduce the cost of the CLWA and make it suitable for mass producation.

2.3.9 Life time

A typical radar warranty is 8000 hours at a mean speed of 37.5 km/h (300000km).

2.3.10 Environmental protection

The protection of the radar components against external environment should not affect their performance. This includes the fragile parts of the CLWA such as the dielectric rod, the silicon substrate and the MEMS switches. In addition, the Radom and the plastic bumper must be transparent regarding the antenna radiation, electromagnetic perturbations, high frequency devices, chocks, thermal aspects, pollution etc.

3 Bibliography

[1] Y. Asano, S. Ohshima, T. Harada, M. Ogawa, and K. Nishikawa. Proposal of millimeter-wave holographic radar with antenna switching. In IEEE MTT-S International Microwave Symposium Digest (Cat. No.01CH37157), volume 2, pages 1111–1114, Phoenix AZ, USA, 2001.